

Cracking and surface oxidation behavior of proton-irradiated type 316 stainless steel in PWR primary water

Yun Soo Lim*, Seong Sik Hwang, Dong Jin Kim, Min Jae Choi, Jong Yeon Lee
Nuclear Materials Safety Research Division/Korea Atomic Energy Research Institute
1045 Daedeok-daero, Yuseong-gu, Daejeon 305-353, Korea
*Corresponding author: yslim@kaeri.re.kr

1. Introduction

Irradiation-assisted stress corrosion cracking (IASCC) of internal components of a pressurized water reactor (PWR) is considered critical for safe long-term operation. Some cracking of internals made of stainless steel (SS), such as guide tube support pins, baffle former bolts and so on, has been identified [1]. The IASCC mechanism is not fully understood; however, it appears to be closely related to microstructural defects caused by neutron irradiation. It is also well known that surface oxidation significantly affects the cracking resistance and cracking behavior. Therefore, studies on microstructural and surface oxidation changes by neutron irradiation should be studied to understand how irradiation defects affect the IASCC behavior of these alloys. Proton irradiation is a useful experimental technique to study irradiation-induced phenomena in nuclear core materials instead of neutrons [2]. Under the proper irradiation conditions, proton irradiation can produce a microstructure and microchemistry very similar to that of neutron irradiation. The objectives of the present work were to investigate the cracking and surface oxidation behavior depending on the radiation dose of proton to obtain clear insight into the role of radiation defects in type 316 SS when exposed to PWR primary water.

2. Methods and Results

2.1 Material and Proton Irradiation

Type 316 austenitic SS was used in this study. The chemical composition of the alloy is given in Tables 1.

Table 1. Composition of the 316 austenitic SS (wt%)

Cr	Ni	C	Mo	Mn	Si	Cu	P	Fe
16.1	10.4	0.047	2.11	1.08	0.66	0.1	0.003	Bal.

The test alloy was solution annealed at 1100 °C and finally water quenched. Before the proton irradiation, the surfaces of the specimens were mechanically ground and then electrochemically polished in a solution of 50 vol% phosphoric acid + 25 vol% sulfuric acid + 25 vol% glycerol for 15 - 30 s at room temperature. The proton irradiation was performed with the General Ionex Tandatron accelerator at the Michigan Ion Beam Laboratory at the University of Michigan. The

irradiation processes were conducted using 2.0 MeV protons at a current range of 40 μ A. The specimens were exposed at 360 °C to four levels of irradiation of 0.4, 1.6, 2.7, and 4.2 displacements per atom (dpa) at a depth of 15 μ m from the surface, which will be referred as A, B, C and D specimens hereafter. It was confirmed from the previous study [2] that the microstructural characteristics of Fe-Cr-Ni alloys proton-irradiated at 360 °C were considerably similar to those neutron-irradiated in operating nuclear power plants. The radiation damage levels of the samples were calculated with the Stopping and Range of Ions in Matter (SRIM) program using a displacement energy of 40 eV in the 'quick calculation' mode.

2.2 SSRT and Surface Oxidation Tests

Slow strain rate test (SSRT) test was conducted using flat tensile specimens to investigate the effect of radiation dose of proton on the IASCC resistance of type 316 SS with a strain rate of 3.4×10^{-7} /s and a total strain of 10 %. The simulated PWR water was prepared prior to the test in a storage tank. 1200 ppm B (by weight) of H_3BO_3 and 2 ppm Li (by weight) of Li(OH) were added to pure water. The oxygen concentration was maintained at less than 5 ppb during the test. The test temperature was 325 °C with a concentration of dissolved hydrogen of 25 $cm^3 H_2/kg H_2O$. Coupons ($10 \times 10 \times 2 mm^3$) for surface oxidation test of the as-received and 2.7 dpa proton-irradiated type 316 SS were prepared by grinding with SiC paper to a 2000 mesh and subsequently polishing with alumina powders down to 0.3 μ m. The test solution chemistry, temperature and the concentration of dissolved hydrogen were identical to those for SSRT test. The oxidation coupons were exposed to the test solutions for a period of 5000 hrs.

2.3 Microstructural Analysis

The focused ion beam (FIB) TEM specimens from the test specimens were prepared using a dual-beam Hitachi FIB-2100 system with Ga ions with an incident beam energy level of 30 kV and a current of 1 - 5 nA. Final thinning was done at an acceleration voltage of 5 kV to eliminate the surface damage produced by highly energetic ions in the early stage of the FIB milling process. The test specimens were investigated using various types of microscopic equipment. A conventional

TEM analysis of the crystallography was conducted with a JEOL JEM-2100F (operating voltage 200 kV). Composition mapping around an oxidation layer was performed by scanning TEM (STEM) electron energy loss spectroscopy (EELS) with a GIF Quantum ER System (Model 965) in an aberration-corrected JEM ARM 200F (operating voltage 200 kV). The energy resolution was 0.3–0.6 eV. STEM EELS was combined with the high-angle annular dark-field (HAADF) technique to produce chemical contrast images formed using electrons diffracted at a high angle (> 40 mrad), with the intensity proportional to the Z atomic number of the elements composing the sample.

2.4 TEM Results on the Irradiation Defects

The irradiation damages depending on the dpa and the depth of 316 SS were calculated with the Stopping and Range of Ions in Matter (SRIM) 2008 program using a displacement energy of 40 eV in the ‘quick calculation’ mode. It was found that the damage profiles exhibited a slow increase roughly up to a depth of $15 \mu\text{m}$, as well as subsequent damage peaks near the depth of $20 \mu\text{m}$ from the irradiated surfaces. Fig. 1 shows a typical dislocation morphology in the as-received type 316 SS before proton irradiation. The dislocation density was quite low due to the high-temperature solution-annealing treatment of $1100 \text{ }^\circ\text{C}$, and the dislocations appeared to be in a straight form. The type 316 SS has a low stacking fault energy; therefore, images due to stacking faults were frequently observed.



Fig. 1. TEM image showing a dislocation morphology in the non-irradiated 316 SS.

Fig. 2 shows dislocations and point defects observed in the 316 SS specimen after proton irradiation with a radiation dose of approximately 4 dpa at a depth of $\sim 16 \mu\text{m}$ from the surface of B specimen. The dislocation density increased considerably by proton irradiation, compared to the density levels in the non-irradiated specimens shown in Fig. 2. An increase in the dislocation density depending on the proton radiation dose was also confirmed in Ni-based Alloy 600 [3]. The types of irradiation defects examined were point defects,

dislocations and voids. Point defects and dislocations were found mainly in the areas exposed to a low radiation dose, whereas voids were dominant in areas exposed to a high radiation dose. More detailed information on the microstructural results of proton-irradiated 316 SS is available in the literature [4].

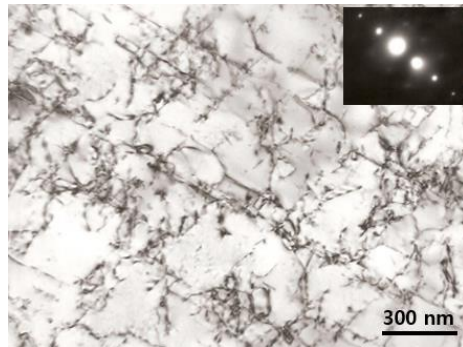


Fig. 2. TEM image showing a dislocation morphology in the proton-irradiated 316 SS with a dose of ~ 4 dpa.

2.5 Effects of proton irradiation on IASCC

The characteristics of microstructural changes by irradiation and their role in changes of material behavior and IASCC have been extensively studied [5]. Irradiation of a material causes hardening, radiation-induced segregation and localized deformation. Uniform elongation is also reduced sharply when a material is irradiated. As such, the alloy becomes significantly embrittled in the PWR operation condition, which in turn makes it much more susceptible to IASCC by irradiation. Fig. 3 shows the cracks found on the surfaces of proton-irradiated tensile specimens after SSRT test at the concentration of dissolved hydrogen of $25 \text{ cm}^3 \text{ H}_2/\text{kg H}_2\text{O}$.

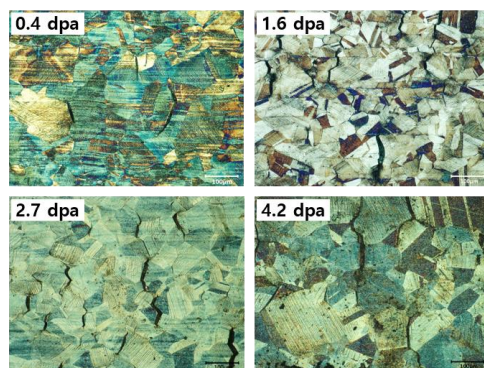


Fig. 3. Cracks found on the proton-irradiated 316 SS after SSRT test at the concentration of dissolved hydrogen of $25 \text{ cm}^3 \text{ H}_2/\text{kg H}_2\text{O}$.

It is evident from Fig. 3 that the crack density and the average size of crack increased as the radiation dose of proton increased [4]. Most of the cracks were found to

propagate along grain boundaries. From the above results, it can be confirmed that proton irradiation significantly increased the IASCC susceptibility in PWR primary water conditions.

2.6 Effects of proton irradiation on surface oxidation

Fig. 4 shows a STEM image, the corresponding HAADF image and EELS composition maps of O, Cr, Fe and Ni around the surface oxidation layer and the grain boundary just beneath the surface of the as-received 316 SS before proton irradiation. The grain boundary in this figure has no intergranular (IG) Cr carbides near the surface; therefore, the reaction of IG Cr carbide with diffused oxygen can be ignored in this case. From the oxygen map of Fig. 4, it can be identified that oxygen diffused into a grain boundary. By oxygen diffusion, Cr and Fe were depleted; however, Ni was enriched on the grain boundary just ahead of the oxidation layer.

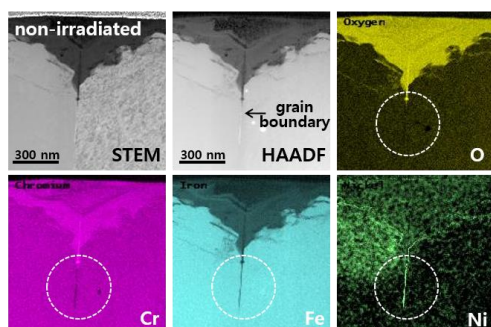


Fig. 4. STEM image, HAADF, and EELS spectrum images of O, Cr, Fe and Ni around the surface oxidation layer and the surface grain boundary of as-received 316 SS.

Fig. 5 shows a STEM image, the corresponding HAADF image and EELS composition maps of O, Cr, Fe and Ni around the surface oxidation layer and the grain boundary just beneath the surface of the 2.7 dpa proton-irradiated 316 SS.

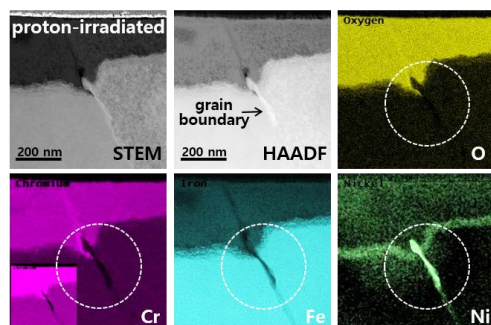


Fig. 5. STEM image, HAADF, and EELS spectrum images of O, Cr, Fe and Ni around the surface oxidation layer and the surface grain boundary of 2.7 dpa proton-irradiated 316 SS.

The grain boundary in this figure was also oxidized due to the oxygen diffusion into the grain boundary. The

remarkable difference of this result from Fig. 4 is that Cr and Fe were more depleted; and Ni was more enriched on the grain boundary just ahead of the oxidation layer, compared to those of non-irradiated 316 SS. The other noticeable thing is, as we can see in the composition maps of Cr and O in Fig. 5, that the grain boundary inside the surface oxidation layer was also oxidized. However, the oxidation of a grain boundary inside the surface oxidation layer was not revealed in the case of non-irradiated 316 SS shown in Fig. 4. All of these changes in surface oxidation behavior might increase the susceptibility to IASCC of proton-irradiated 316 SS. Much more research on surface oxidation phenomena appears to be necessary to obtain clear insight into IASCC resistance and behavior of the proton-irradiated 316 SS.

3. Conclusions

Type 316 SS samples were irradiated using 2 MeV protons with an average dose rate of $\sim 7.1 \times 10^{-6}$ dpa/s at 360 °C. The various irradiation defects, IASCC susceptibility and the surface oxidation behavior induced by proton irradiation were characterized. The types of irradiation damage examined were point defects, dislocations and voids. Point defects and dislocations were found mainly in the area exposed to a low radiation dose; however, voids were dominant in areas exposed to a high radiation dose. The crack density and the average size of crack increased as the radiation dose of proton increased, and the surface oxidation phenomena were changed by proton irradiation. All of the microstructural and surface oxidation changes induced by irradiation degrade the mechanical properties of a material and appear to significantly reduce the resistance to IASCC of structural components installed near the core region of a PWR.

REFERENCES

- [1] J. McKinley, R. Lott, B. Hall and K. Kalchik, Examination of Baffle-Former Bolts from D.C. Cook Unit 2, Proc. of the 16th Int. Conf. on Environmental Degradation of Materials in Nuclear Power Systems-Water Reactor, 2013.
- [2] J. Gan and G.S. Was, Microstructure Evolution in Austenitic Fe-Cr-Ni Alloys Irradiated with Protons: Comparison with Neutron-Irradiated Microstructures, Journal of Nuclear Materials, Vol.297, p. 161, 2001.
- [3] J.-J. Kai and R.D. Lee, Effects of proton irradiation on the microstructural and microchemical evolution of Inconel 600 alloy, Journal of Nuclear Materials, Vol.207, p.286, 1993.
- [4] Y.S. Lim, S.S. Hwang, D.J. Kim, M.J. Choi, J.Y. Lee, Microstructural Characterization of Proton-Irradiated Type 316 Stainless Steel, Trans. Kor. Nucl. Soc. Spring Meeting, Jeju Korea, May 23-24, 2019
- [5] G.S. Was, S.M. Brummer, Effects of Irradiation on Intergranular Stress Corrosion Cracking, Journal of Nuclear Materials, Vol.216, p. 326, 1994.